

# Shape Selection in Chiral Self-Assembly

Robin L. B. Selinger,<sup>1,2</sup> Jonathan V. Selinger,<sup>1</sup> Anthony P. Malanoski,<sup>1</sup> and Joel M. Schnur<sup>1</sup>

<sup>1</sup>*Center for Bio/Molecular Science and Engineering, Naval Research Laboratory,  
Code 6900, 4555 Overlook Avenue, SW, Washington, DC 20375*

<sup>2</sup>*Physics Department, Catholic University of America, Washington, DC 20064*

(Dated: March 10, 2004)

Many biological and synthetic materials self-assemble into helical or twisted aggregates. The shape is determined by a complex interplay between elastic forces and the orientation and chirality of the constituent molecules. We study this interplay through Monte Carlo simulations, with an accelerated algorithm that simulates the growth of an aggregate out of solution. The simulations show that the curvature changes smoothly from cylindrical to saddle-like as the elastic moduli are varied. Remarkably, aggregates of either handedness form from molecules of a single handedness, depending on the molecular orientation.

A wide range of materials self-assemble into chiral aggregates. These include biological materials and their synthetic analogues, such as carbohydrate- [1] and amino-acid-based amphiphiles [2], peptides [3, 4], diacetylenic lipids [5, 6], gemini surfactants [7], and multicomponent mixtures in bile [8, 9]. Aggregates form as bilayer membranes in solution, and grow into a range of chiral shapes, including tubules with “barber-pole” markings, helical ribbons with cylindrical curvature, and twisted ribbons with Gaussian saddle-like curvature [10]. They form through a variety of pathways, including reorganization of large spherical vesicles and growth directly out of solution [11].

While one might expect that macroscopic handedness of an aggregate is tied to the molecular-scale chirality of its constituents, experiments have shown that the relationship is not always that simple. In the early stages of self-assembly, diacetylenic lipids can form both right- and left-handed helical ribbons, even though the equilibrium state has tubules of a uniform handedness [12]. In a biological analogy, chirality reversal at the organism level arises occasionally via genetic mutations, and has been observed in plants, molluscs, birds, and mammals, even though the proteins and other molecules within each organism retain their normal chirality [13, 14, 15].

Experiments have also shown that the relationship between material properties and the macroscopic shape of chiral aggregates is surprisingly complex. For example, charged gemini surfactants with chiral counterions exhibit a transition between helical ribbons with cylindrical curvature and twisted ribbons with Gaussian curvature as a function of molecular chain length [7]. Similarly, mixed bilayers of saturated and diacetylenic phospholipids show transitions from micron-scale cylindrical tubules to twisted ribbons, and then to nanometer-scale tubules, as a function of temperature [16].

To understand the shape of chiral aggregates, and to design new structures for nanotechnology, we must learn how to control aggregate size and shape by adjusting the chemical composition and the conditions under which self-assembly occurs. An important step toward this goal is to understand how the membrane’s elastic moduli,

chirality, and tilt orientation together control the structure of the resulting aggregate. Earlier theoretical models have studied this by using continuum elastic theory to calculate the energy of twisted membranes in simple geometries [17]. Such models show that chiral interactions, coupled with molecular tilt, lead to the formation of cylindrical tubules or helical or twisted ribbons. The limitation of this analytical approach is that it considers only idealized structures, and does not explore the full range of potential shapes or the mechanism of shape transitions. Finite-element modeling of membranes and vesicles would allow free exploration of shapes, but no such models have taken the membrane’s molecular tilt and chiral interactions explicitly into account. Molecular-scale simulation of tilted bilayer membranes is another possible approach [18], but available system sizes are too small to allow studies of shape selection.

In this paper, we present a new mesoscale simulation approach to explore the roles of elasticity, chirality, and molecular tilt in chiral self-assembly. We develop an accelerated technique that simulates the growth of an aggregate out of solution, and allows the aggregate to select its shape through a Monte Carlo process. This approach provides an explicit visualization of a range of possible shapes, and shows that the aggregate shape varies smoothly from cylindrical to Gaussian curvature as the elastic properties of the membrane are varied. Moreover, it shows that the handedness of the aggregate depends on the orientation of molecular tilt as well as on the handedness of the chiral interactions, demonstrating one mechanism by which both right- and left-handed structures can form from a material of uniform molecular chirality.

In our mesoscale approach, a chiral elastic ribbon is modeled as a tethered membrane composed of interaction sites connected by elastic springs to form a triangular lattice, as shown in Fig. 1. Each interaction site represents a small “patch” of membrane. The membrane can deform in three-dimensional (3D) space, so that each site has position  $\mathbf{r}_i$ , and local upward normal  $\mathbf{n}_i$ . The local molecular orientation at each site is described by the director  $\mathbf{d}_i$ , a vector of unit length. This approach is analogous to earlier studies of tethered membranes [19],

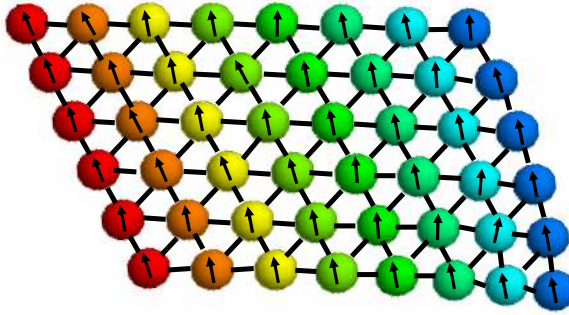


FIG. 1: (Color online) Model of a chiral elastic ribbon as a tethered membrane composed of interaction sites connected by elastic springs to form a triangular lattice. The local molecular orientation at each site is described by a director, as indicated by the arrows.

but here the membrane has the additional features of chirality and molecular orientation. It is also analogous to mesoscale models of smectic liquid crystals, which have chirality as well as a molecular orientation defined on a lattice [20], but here the membrane is free to change its shape in 3D. In our initial exploration of the model, we constrain the director on each site at a typical experimental tilt angle of  $30^\circ$  with respect to the local upward normal  $\mathbf{n}_i$ , with the tilt oriented along the ribbon's long edge, which is also along a bond between neighboring sites. In future work we will remove this constraint and consider the possibility of modulated membrane tilt.

To investigate shape selection, we must define a model for the elastic energy of a chiral membrane that takes into account the microscopic chirality of its constituent material. We use a lattice expression analogous to the continuum energy for chiral membranes investigated in earlier work [17]. It includes a chiral elastic term as well as bend, stretch, and hard-core contributions:

$$E = \sum_{\langle i,j \rangle} \left[ \lambda (\mathbf{d}_i \times \mathbf{d}_j) \cdot \frac{(\mathbf{r}_i - \mathbf{r}_j)}{|\mathbf{r}_i - \mathbf{r}_j|} - K_{\text{bend}}(\mathbf{n}_i \cdot \mathbf{n}_j) \right. \\ \left. + \frac{1}{2} K_{\text{stretch}} (|\mathbf{r}_i - \mathbf{r}_j| - R_0)^2 \right] \\ + \sum_i \sum_j U_{\text{hc}} (|\mathbf{r}_i - \mathbf{r}_j|) \quad (1)$$

In the first term of this expression, the chiral elastic parameter  $\lambda$  gives an energetic preference for twisting the directors  $\mathbf{d}_i$  and  $\mathbf{d}_j$  away from parallel alignment. Reversing the sign of  $\lambda$  reverses the favored chiral twist of the director field. In the second term, the parameter  $K_{\text{bend}}$  controls the energy of bending the membrane so that the local normal vectors on sites  $i$  and  $j$  are not parallel. In the third term, the Hooke's law constant  $K_{\text{stretch}}$  gives the energy of separating sites  $i$  and  $j$  away from their equilibrium separation  $R_0$ . In those three terms, the sum on  $\langle i,j \rangle$  refers to all nearest-neighbor pairs of sites in the membrane. The final term in the energy rep-

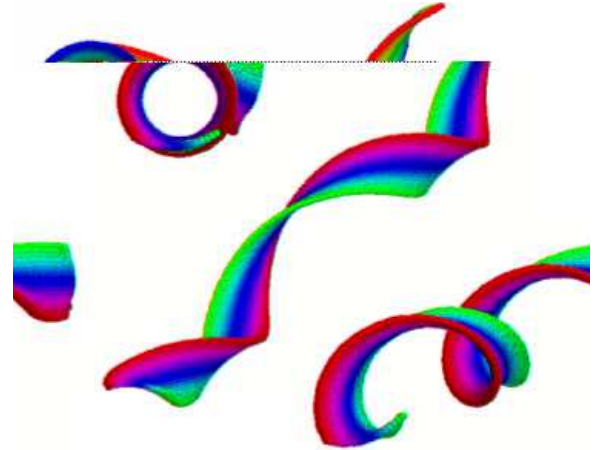


FIG. 2: (Color online) Three views of a helical ribbon, showing the 3D structure. The ribbon has grown to a size of  $16 \times 216$  sites.

resents a hard-core potential between any pair of sites, with  $U_{\text{hc}}(r) = 0$  for  $r > a$ , and  $U_{\text{hc}}(r) = \infty$  for  $r \leq a$ , where  $a = \frac{2}{3}R_0$  is the hard-core diameter. That term prevents the membrane from intersecting itself.

For Monte Carlo simulations of the membrane, we need a simulation algorithm that will come to equilibrium in a reasonable time. For a first attempt, we initialized the system as a long, flat ribbon, and allowed it to evolve via off-lattice Monte Carlo simulation with the Metropolis algorithm. However, we found that this process evolves much too slowly to reach a twisted shape, because the twist must start at the ribbon's narrow ends and diffuse inward toward the middle. With only single-particle Monte Carlo steps, the equilibration time grows sharply with the ribbon length. Coordinated multi-particle moves such as application of overall twist to the membrane could accelerate equilibration, but there is a risk that such moves might introduce a bias into the shape selection process.

For an alternative simulation approach to facilitate rapid relaxation to an equilibrium state, we simulate the growth of a chiral aggregate out of solution. We start the system as a small ribbon of size  $16 \times 16$  sites, and then add new rows one at a time up to a maximum size of  $16 \times 216$  sites. After each row addition, the last 8 rows are equilibrated for 10,000 Monte Carlo steps per site, and then the whole ribbon is equilibrated for an additional 5000 Monte Carlo steps per site. The concept of simulating a growth process has found wide application in the study of polymers [21, 22], but this is its first application to chiral membranes. The temperature is kept near zero so that the Monte Carlo process is essentially an energy minimization, which allows comparison with previous analytical results. In future work we will address the role of thermal fluctuations in membrane shape. An example of a chiral membrane grown in this fashion is shown in Fig. 2, and animations of the growth are presented in EPAPS [23]. In the figures and animations, colors are a

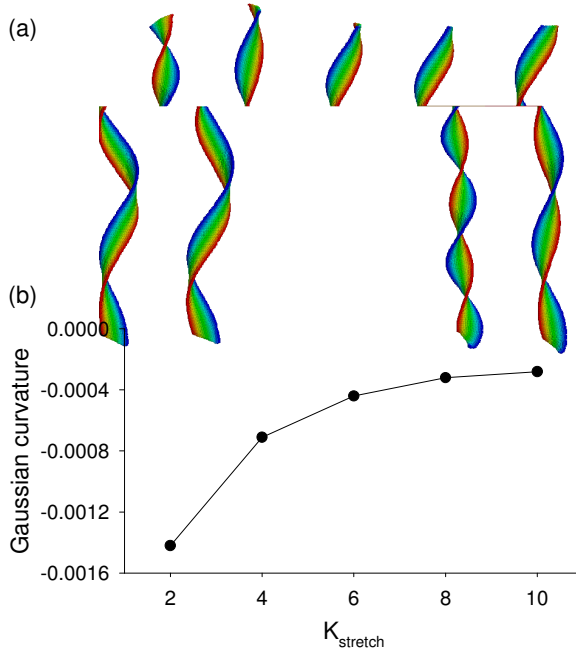


FIG. 3: (Color online) (a) Series of ribbons grown with the parameter  $K_{\text{stretch}} = 2, 4, 6, 8$ , and 10, showing the crossover from twisted ribbons with Gaussian saddle-like curvature to helical ribbons with cylindrical curvature. (b) Plot of the Gaussian curvature for the five ribbons, calculated at the central point of the ribbons, in units of the hard-core diameter  $a^{-2}$ . This plot confirms that all of the structures have some Gaussian curvature, and that the level of Gaussian curvature changes gradually as a function of the elastic parameters.

guide to the eye to visualize the 3D structure.

We use this simulation approach to investigate how the final equilibrium shape of the aggregate depends on membrane properties. Of the three elastic parameters  $K_{\text{stretch}}$ ,  $K_{\text{bend}}$ , and  $\lambda$ , it is necessary to vary two since only their ratios are significant at low temperature. We begin by examining the effect of varying the stretch modulus  $K_{\text{stretch}}$  over a range from 2 to 10 in arbitrary units, while  $K_{\text{bend}} = 1$  and  $\lambda = 1$  are held fixed. We observe the gradual structural transition shown in Fig. 3(a). For low  $K_{\text{stretch}}$ , we find a twisted ribbon with Gaussian saddle-like curvature, while for high  $K_{\text{stretch}}$ , the shape is a helical ribbon with cylindrical curvature. This transition is physically reasonable, because Gaussian curvature requires stretching the membrane, which is suppressed by  $K_{\text{stretch}}$ . The small Gaussian curvature that remains in helical ribbons for high  $K_{\text{stretch}}$  resembles the ripple structure that has been predicted theoretically [24].

We have done an analogous study of the effects of varying the bend modulus  $K_{\text{bend}}$ . We fix  $K_{\text{stretch}} = 6$  and  $\lambda = 1$ , and vary  $K_{\text{bend}}$  over the range from 1 to 2.4. The simulation results (not shown) give a similar gradual transition from helical ribbons at low  $K_{\text{bend}}$  to twisted ribbons at high  $K_{\text{bend}}$ .

Each structure is characterized by a radius, a pitch, and two curvature parameters. Through the structural

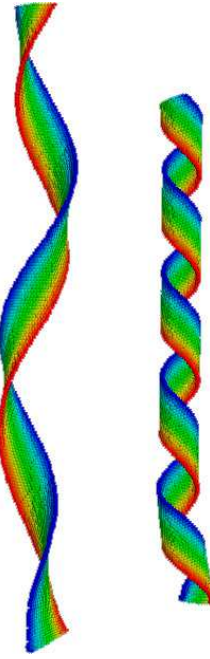


FIG. 4: (Color online) Two ribbons grown with the same elastic parameters, but with different orientations of the director representing the molecular tilt. In the left case, the tilt is aligned along the long axis of the ribbon, but in the right case it is aligned along the short axis. This change in the tilt direction reverses the handedness of the ribbon, and greatly changes the radius and pitch.

transition shown in Fig. 3(a), all of these measures show a continuous and gradual transition. In particular, note that none of the structures are ideal twisted or helical ribbons with pure Gaussian or cylindrical curvature. Rather, each structure involves a combination of Gaussian and cylindrical curvature, and the combination changes gradually as a function of  $K_{\text{stretch}}$ . We can calculate the Gaussian curvature at any interaction site by adding up the six incident bond angles  $\theta_i$  at that site. If the Gaussian curvature is zero, then the six bond angles add up to  $2\pi$ . Hence, the deviation of the sum away from  $2\pi$  is a simple measure of the Gaussian curvature [25, 26]:

$$\kappa_{\text{Gauss}} = \frac{3 \left( 2\pi - \sum_{i=1,6} \theta_i \right)}{\sum_{i=1,6} a_i}, \quad (2)$$

where  $a_i$  are the areas of the triangles adjacent to the site. Figure 3(b) plots the Gaussian curvature of each ribbon shown in Fig. 3(a), evaluated at the central point of the ribbon, as a function of  $K_{\text{stretch}}$ . The variation in Gaussian curvature is very substantial, ranging over a factor of 5. However, it does not occur as a sharp structural transition, but rather as a smooth crossover.

To further investigate this model, we explore the con-

sequences of changing the molecular tilt direction in the membrane. In the original simulations, the director was constrained to point along the ribbon's long edge, along a bond between neighboring interaction sites (as in a smectic-*I* liquid crystal). We now rotate it by 90° to point perpendicular to the long edge, halfway between two nearest-neighbor bonds (as in a smectic-*F* liquid crystal). Although the sign and magnitude of the membrane's chiral interaction parameter  $\lambda$  remain unchanged, the handedness of the aggregate switches from right- to left-handed, as shown in Fig. 4. The pitch and diameter of the aggregate also change greatly.

While somewhat counter-intuitive, the handedness reversal is physically reasonable. Earlier theoretical work showed that the curvature direction favored by molecular chirality is 45° from the tilt direction [17], so rotating the tilt direction by 90° should change the curvature direction by 90°, giving a handedness reversal. (As a thought experiment, we can imagine cutting a cylindrical tubule to form a helical ribbon. If we cut it along the tilt direction, the ribbon has one handedness. If we cut it perpendicular to the tilt direction, the ribbon has the opposite handedness.) This result shows that aggregates may form with either handedness even from enantiomerically pure material, simply by variation of the molecular tilt direction with respect to the edges. This could be a possible explanation of the experiments on conflicting handedness mentioned earlier [12].

The change in pitch and diameter is a more subtle effect, which we cannot attribute to the change in tilt direction relative to the ribbon's long edge. Rather, it

is probably due to changing the tilt direction relative to the nearest-neighbor bonds in the membrane. This change can greatly modify the elastic properties of the membrane, which would alter the geometric parameters of the resulting aggregate. This result shows that aggregates can have different pitch and diameter even if they are composed of the same material, just by variation of the tilt direction with respect to the crystallographic axes. This could be a possible explanation of the different geometric structures seen in bile [8, 9].

In conclusion, we have developed an accelerated approach for studying the shapes of chiral aggregates through Monte Carlo simulation of a growth process. The simulation results show that a short-range chiral interaction leads to the formation of complex chiral shapes, which undergo a gradual crossover between Gaussian saddle-like curvature and cylindrical curvature as a function of the interaction parameters. The handedness of the macroscopic shapes is determined by the interplay between the microscopic chiral energetic parameter and the orientation of the molecular tilt. Thus, this work shows the range of shapes that occur in experimental studies of chiral self-assembly, provides a possible explanation for experiments on conflicting handedness, and demonstrates an approach for future simulations based on even more detailed microscopic models of chiral molecular structure.

This work was supported by the Office of Naval Research and the National Science Foundation Grant No. DMR-0116090. APM was supported by a fellowship from the National Research Council.

---

[1] B. Pfannmüller and W. Welte, *Chem. Phys. Lipids* **37**, 227 (1985).  
[2] N. Nakashima, S. Asakuma, J. M. Kim, and T. Kunitake, *Chem. Lett.* 1709 (1984).  
[3] S. G. Zhang, T. Holmes, C. Lockshin, and A. Rich, *Proc. Natl. Acad. Sci. U.S.A.* **90**, 3334 (1993).  
[4] A. Aggeli *et al.*, *Nature* **386**, 259 (1997).  
[5] P. Yager and P. E. Schoen, *Mol. Cryst. Liq. Cryst.* **106**, 371 (1984).  
[6] For a review, see J. M. Schnur, *Science* **262**, 1669 (1993).  
[7] R. Oda *et al.*, *Nature* **399**, 566 (1999).  
[8] D. S. Chung, G. B. Benedek, F. M. Konikoff, and J. M. Donovan, *Proc. Natl. Acad. Sci. U.S.A.* **90**, 11341 (1993).  
[9] Y. V. Zastavker *et al.*, *Proc. Natl. Acad. Sci. U.S.A.* **96**, 7883 (1999).  
[10] For a review, see M. S. Spector, J. V. Selinger, and J. M. Schnur, in *Materials-Chirality: Volume 24 of Topics in Stereochemistry*, edited by M. M. Green, R. J. M. Nolte, and E. W. Meijer (Wiley, Hoboken, 2003), p. 281.  
[11] M. S. Spector, J. V. Selinger, and J. M. Schnur, *J. Am. Chem. Soc.* **119**, 8533 (1997).  
[12] B. N. Thomas, C. M. Lindemann, and N. A. Clark, *Phys. Rev. E* **59**, 3040 (1999).  
[13] I. Soulié-Mär sche, in *Advances in BioChirality*, edited by G. Pályi, C. Zucchi, and L. Caglioti (Elsevier, Amsterdam, 1999), pp. 191-207.  
[14] R. Ueshima and T. Asami, *Nature* **425**, 679 (2003).  
[15] M. Levin and M. Mercola, *Genes and Development* **12**, 763 (1998).  
[16] M. S. Spector, A. Singh, P. B. Messersmith, and J. M. Schnur, *Nano Letters* **1**, 375 (2001).  
[17] For a review, see J. V. Selinger, M. S. Spector, and J. M. Schnur, *J. Phys. Chem. B* **105**, 7157 (2001).  
[18] For example, see C. Hofsäß, E. Lindahl and O. Edholm, *Biophys. J.* **84**, 2192 (2003).  
[19] Y. Kantor, M. Kardar, and D. R. Nelson, *Phys. Rev. Lett.* **57**, 791 (1986); *Phys. Rev. A* **35**, 3056 (1987).  
[20] For example, see J. V. Selinger *et al.*, *Phys. Rev. E* **62**, 666 (2000).  
[21] M. N. Rosenbluth and A. W. Rosenbluth, *J. Chem. Phys.* **23**, 356 (1955).  
[22] D. Frenkel and B. Smit, *Understanding Molecular Simulation* (Academic Press, San Diego, 1996).  
[23] See EPAPS for animations of the simulated growth of chiral elastic ribbons, starting with a size of 16 × 16 sites, and growing to a size of 16 × 216.  
[24] J. V. Selinger, F. C. MacKintosh, and J. M. Schnur, *Phys. Rev. E* **53**, 3804 (1996).  
[25] T. Regge, *Il Nuovo Cimento* **19**, 558 (1961).  
[26] C. Lin and M. J. Perry, *Proceedings, IEEE Workshop*

on Computer Vision: Representation and Control, 38  
(1982).